Heliyon 10 (2024) e33587

Contents lists available at ScienceDirect

Heliyon

journal homepage: www.cell.com/heliyon

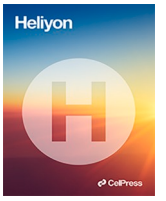

Research article

Spatiotemporal variability and trends in rainfall and temperature extremes using ERA5 reanalysis and CORDEX–Africa model in Southern Ethiopia

Zewde Sufara Yagaso *, Teshome Yirgu Bayu, Mulugeta Debele Bedane

Department of Geography and Environmental Studies, College of Social Sciences and Humanities, Arba Minch University, Arba Minch, Ethiopia

ARTICLE INFO

Keywords:
Climate model
Climate variability
Cool night
Modified mann-kendall test
Warmest day

ABSTRACT

Rainfall and temperature are characterized by spatial and temporal variability in Ethiopia. However, less attention was given for the analysis of climate variability using advanced techniques and multiple sets of data. This study was conducted to examine spatiotemporal variability and trends in rainfall and temperature extremes in Ghibe III Dam watershed. Observational, ERA5, and regional simulation model data sets were used. The coefficient of variation (CV) and precipitation concentration index (PCI) were employed. The trends in rainfall and temperature extremes were examined using the modified Mann-Kendall test and the Sen Slope estimator in *R*-ClimDex in R 4.2.2 software. The warmest days exhibited temperature from *24.6*°C *to 40*°C *in Bele, 28.2*°C *to 35.43*°C *in* Wolaita Sodo, 33.6 °C–44 °C in Areka, 31.64 °C–36.8 °C in Gesuba, and 29.19 °C–36.15 °C in Gena Bosa. The warmest nights showed temperature ranging from 14 °C to 18.74 °C in Bele and Gena Bosa, respectively. Annual warm days (TX90p) ranges from 11.34 to 57.1 days, with higher heating in the southern parts. The cool days (TX10p) range from 2.79 to 8.41, while the cool nights (TN10p) range from 0.04 to 8.26 days. The areal average temperature maximum and minimum range between 26.37 °C and 13.81 °C, respectively, with mean precipitation of 1446.92 mm.The rainfall extremes indices showed increasing and decreasing trends. The extreme temperature indices showed an overall warming trend. Based on ERA estimates, the rainfall in winter showed higher variability (CV = 72.4%–99.3 %) than the annual rainfall (CV = 33%–79.8 %). PCI showed a moderately (12 %) to very erratic (19.4 %) rainfall distribution. The climate model estimate showed high variability (CV = 20.65 %) in Climate Limited Area Modeling Community (CCLM) under representative concentration paths (RCP) 4.5 and 8.5 and extremely high variability (CV = 93.49 %) in the Regional Atmospheric Climate Model (RACMO) under RCP 4.5. Policymakers should design appropriate adaptation strategies applicable to farmers.

1. Introduction

Africa is susceptible to the effects of climate variability for the fact that its economy depends on rainfed agriculture and 75 % of its part found in tropical zone characterized by fluctuating temperature and rainfall extremes [1–3]. Birara et al.and Zegeye et al. [4,5] figured out that Ethiopia is one of the low-income countries with less capacity of adaptation in Africa vulnerable to the adverse effects

* Corresponding author.
E-mail addresses: sufarayagaso2015@gmail.com, zewdes2021@gmail.com (Z.S. Yagaso).

https://doi.org/10.1016/j.heliyon.2024.e33587
Received 6 May 2023; Received in revised form 7 June 2024; Accepted 24 June 2024
Available online 25 June 2024

of climate change and variability. The climate variability occurs mostly at monthly and seasonal scales than it does on an annual basis in the country according to Worku et al. [6].

The extreme events are commonly happening in many parts of Ethiopia. For instance, Gummadi et al. [7]reported that the consecutive wet days(CWD) decreased while the consecutive dry days (CDD) increased in Eastern and South Eastern parts of the country during rainy (summer and Spring) seasons. The rainfall and temperature extreme events are inflicting agricultural productivity recurrently in Ethiopia. The extremes theory or the theory of large deviation is about the mathematical framework that describes the occurrence of rare or extreme events [8,9]. Grounding climate variability study on the extreme theory helps to understand the extent, magnitude, probability, characteristics, and frequency of climate extremes so that understanding can be reached to develop better adaptation strategies and actions to be taken on the extreme events happening. Nevertheless, Jothimani et al. and Wubaye et al. [10,11] showed that the extremes of climate caused by variability have not been the focus of many studies in Ethiopia.

Climate variability affects agriculture which is the backbone of the Ethiopian economy so local-level investigation like the current study is crucial to developing site-specific adaptations to ensure sustainable agriculture as suggested by Alemayehu et al. [12] as variability and trends in rainfall and temperature are highly contextualized in the country.

The scarcity of climate data also limits the process of characterizing the rainfall and temperature in Ethiopia. Like various parts of the country, the current study area is characterized by inconsistent, insufficient, and inaccurate as well as a dearth of meteorological data to evaluate variability and trends in rainfall and temperature.

Besides, previous studies showed various contradicting results in variability and trend analyses in the Ethiopia [12–15] which necessities further study to reduce the effects of climate variability.

Several studies [2,13,14,16,17] also focused on the classic Mann-Kendall test and Sen slope estimator and only observational for analysis of spatiotemporal variability and trends of rainfall and temperature. The Mann-Kendall test is not free from autocorrelation. However, it is modified Mann-Kendall test which is free of autocorrelation according to Koudahe et al. [18]. Thus, few studies employed the Modified Mann-Kendall test to analyze the trends of rainfall and temperature in Ethiopia.

The use of observational data, ERA5 and CORDEX Africa data sets in integration was rare. Kawo et al. [19] indicated that ERA 5 data set provides the daily rainfall and temperature minimum and maximum and is important due to its closeness to the observational data and easily be available at 0.25° x 0.25° spatial resolution thus, serving as a substitute in countries where weather-ground based data are scarce. The European Centre for Medium-Range Weather Forecasts (ECMWF) provides ERA5, an atmospheric reanalysis of the global climate based on satellite measurements. Besides, McNicholl et al. [20] showed that ERA 5 is a replacement for ERA-Interim that performs better and provides time series data on temperature and rainfall with high spatial and temporal resolutions. Thus, ERA5 was opted for current study as gap filling in shortage of meteorological data. Shongwe et al. [21] stated that CORDEX-Africa provides data with resolution of 0.44° useful for forecasting the future and quantifying uncertainties. Ethiopia is located among three CORDEX domains, hence CORDEX Africa models like CCLM, RACMO, RCA4, and REMO were chosen for this study, as proposed by Van Vooren et al. [22]. Therefore, there was a gap in existing literature in characterizing rainfall and temperature using multiple sets of data rather depending on single data sets together with the use of classic Mann-Kendall test.

The climate has not better characterized and awareness was not created among agrarian communities, the rainfed agriculture as it is the dominant economic activity is threatened endangering the livelihood of the people in current study area. Therefore, analyzing variability and trends in rainfall and temperature and the use of integrated data sets as well as modified Mann-kendall test fills the gap in the literature and the use of integrated data sets and modified Mann-Kendall test have been given less attention in scientific literature. Hence, using climate model data, ERA5 reanalysis, and the available meteorological data may reduce the issue of inaccurate gauge station data and help better characterize rainfall and temperature in the area so that it is possible to understand the variability and trend in rainfall and temperature.

The study would be helpful for policymakers providing baseline information to make informed decisions and for small-scale farmers to choose appropriate area-specific adaptation strategies. The international community would benefit from the knowledge acquired from this study in which climate studies require the integration of multiple data sets and related factors other than using only a single faceted data set, which does provide complete picture of current climatic phenomena.

The study has significance for scientists and researchers in the field of hydrology, water, and food security. For instance, hydrologists can understand the effects of climate change on hydrological process. Scientists would be initiated for further studies on the adverse effects of climate variability on water availability, stream flows, and water volumes, surface, and sub-surface water so that it can shed light on the possible effects of variability and trends in rainfall and temperature on the water resource, urging planners to create strategies for adaptation. Designing climate-smart agriculture requires an understanding of the local climate characteristics. As a result, it contributes to the development of a climate-resilient economy that is resistant to drought.

To combat the negative consequences of climatic variability, adaptation strategies can be developed with the help of climate research. Thus, scientifically, the current study is significant to know climate change pattern, understand future climate by examining spatiotemporal patterns based on the ERA 5 and CORDEX climate models; inform rural communities about the changing characteristics and trends of rainfall and temperature to develop adaptation strategies since the extremes events have an impact on agricultural productivity. Additionally, the study would help reduce the risk that may occur due to extreme climate events by taking action and establishing the culture early warning systems.

To our knowledge is concerned and based on readings of many literatures, the effects of fluctuating rainfall and temperature were challenges in the past, present, and continue to threaten the livelihoods of communities in the world. Therefore, to better take action and revise the existing strategies and implementation levels, characterizing rainfall and temperature by integrating multiple data from various sources and using recent techniques of analysis have great importance for the international community. Therefore, this study was conducted to analyze spatiotemporal variability and trends in rainfall and temperature in the Ghibe III Dam watershed, Middle

reaches of Omo basin, Southern Ethiopia.

2. Materials and methods

2.1. Description of the study site

Ghibe III Dam watershed is part of the Omo-Ghibe River Basin in Ethiopia which is the country's second-largest basin, encompassing an area of about 79,000 sq. km and is drained by two large rivers: the Ghibe River, which flows south, and the Gojeb River, which flows from west to east and at their confluence named as Omo River. It is an enclosed river basin that drains into Lake Turkana between Kenya and Ethiopia, bordered on the west by the Baro-Akobo Basin, on the north and northwest by Blue-Nile Basin, on the northeast by Awash Basin, and the eastern side by the Rift Valley Lakes Basin according to Bekele et al. and Jaweso et al. [23,24]. Jaweso et al. [23] clarified that the Omo basin has a variety of topographic features ranging from 746 m. a.s.l in the southern to 3522 m. a.s.l in the northern highlands. The mean annual precipitation was 1425 mm, with the wet season (March to October) receiving 92 % of it and the dry season (November to February) only receiving 8 %. The Ghibe III Dam watershed which the current study area covers extends from 6°36′0″ to 6°57′0″N and $37^{0}0'0''$E to 37,°31′30″E and is found in the middle reaches of the Omo River (Fig. 1) where Bota, Koma, Debi, Worera, Gamo Dimaye, Bele, Arfine, and Legiche drain Kindo Koisha woreda, and Dola, Yawara, Xingle, Yeguwa, Gindra, Kareta, and Ugumane drain Loma Bosa Woreda and the tributaries from either sides join Omo river according to Girma et al. [25]. The materials of this study included observed data from National meteorological agency of Ethiopia, ERA5 Reanalysis, CORDEX data sets, CMhydra, R package, ClimDex, Origin pro-2019, excel and Arc GIS tools.

2.2. Data source and definition of temperature and precipitation variables

Température, or more specifically, the potential for heat transmission, is the measure of how "hot" a body is while rainfall is the amount of rain that falls in an area during a period when water vapor in the atmosphere condenses into droplets that can no longer be suspended in the air as explained by Selase et al. [26]. The daily rainfall and température observed data for Bele, Gassachere, Wolaita Sodo, Areka, Gessuba, and Gena Bosa were collected from the National Meteorological Agency of Ethiopia from 1990 to 2021. For bias correction, Bele and Gassachere stations' rainfall and température data were used due to their presence in the heart of the Watershed in relation to other stations in and around the study area. The régional climate model (RCM) was localized to the study area by using the coordinates of Bele and Gassachere stations. Additionally, the Regional Climate Model (RCM), CORDEX-Africa model (Table 1), and ERA5 data were employed.

Regional climate models were employed to understand the past, present and future variability and trends in rainfall and temperature in the watershed. As a result of the inadequacy of gauged stations with long period of time and complete data. ERA5 was also used where nine locations in and around the Ghibe III dam Watershed were selected and the daily rainfall and temperature data were collected. Using the daily rainfall and temperature data of Bele (1990–2005) and Gassachere (1999–2007) stations, the ERA 5 and climate model data were examined and bias-corrected before the analysis. Gassachere station was taken only for the Climate model and

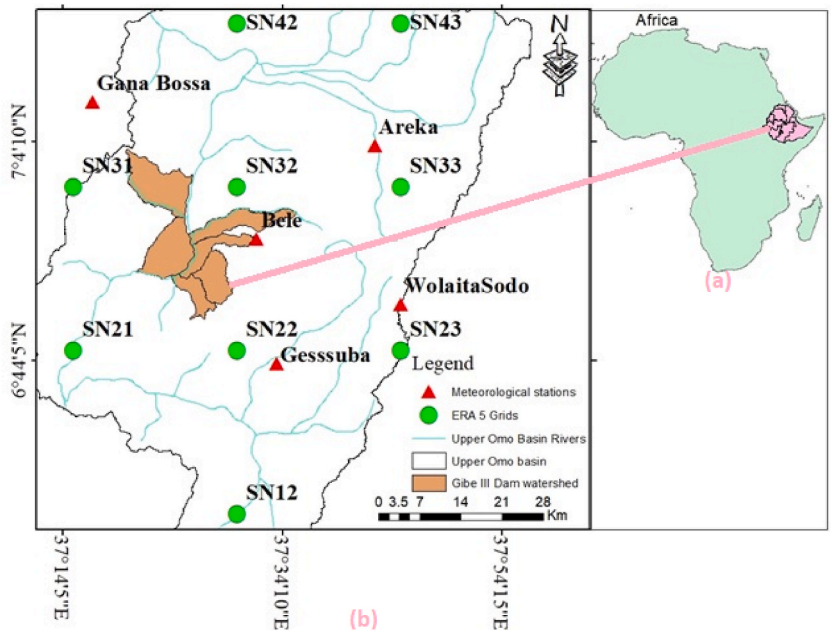

Fig. 1. Map of the study area (a) and (b).

Table 1
Regional climate models used in Ghibe III Dam watershed (1990–2021).

No	Regional climate model	Full Name	Founding Institution	Reference
1	RCA4	SMHI Rossby Center Regional Atmospheric model (RCA4)	Swedish Meteorological and Hydrological Institute, Rossby Centre, Sweden	Jones et al. [27]
2	CCLM	CLMcom COSMO-CLM(CCLM) version 4.8	Climate Limited Area Modeling Community (CLMcom), USA	Sørland et al. [28].
3	RACMO22T	KNMI Regional Atmospheric Climate Model, version 2.2(RACMO2.2T)	Koninklijk Nederland's Meteorologists Institute (KNMI), Netherlands	van Meijgaard et al. [29].
4	REMO 2009	MPI regional model (REMO)	Max Planck Institute (MPI), Germany	Jacob et al. [30]

ERA 5 data bias correction together with Bele station, however, it was excluded from meteorological stations that were used to analyze the observed climate data. This was because, of course, it is in the heart of the Ghibe III Dam watershed, but characterized by the incompleteness of data of temperature and rainfall.

Thus, based on meteorological data of Bele, Wolaita Sodo, Areka, Gena Bosa, and Gessuba stations, the variability and trends in rainfall and temperature extremes were examined using the modified Mann Kendall trend test in R 4.2.2 software. The spatiotemporal variability of rainfall and temperature were analyzed using the coefficient of variation and precipitation concentration index based on ERA 5 data. The ERA5 reanalysis has an advantage because it integrates several factors including rainfall and temperature and has a high resolution, which is appropriate for this current investigation unlike chirp, which just provides rainfall. ERA5 better represents the interannual variability by reducing biases in temperature and precipitation in most of Africa. Moreover, Gleixner et al. [31] have reported that in extreme years, ERA5 better depicts the spatial distribution of precipitation. Despite ERA5's slightly better performance in terms of capturing observed long-term trends than ERA-interim, the reanalysis product performed poorly in terms of capturing observed long-term trends. However, there was no other options to use ERA5 as there were no adequate meteorological stations in the present study area. Thus, following an evaluation of the efficiency of satellite products in East Africa by scholars [31,32] and evaluating its performance using observed data of Bele and Gassachere stations, ERA 5 data for 9 locations (Table 2) were used in this study. At some locations from nine grids, ERA5 estimates were compared to the meteorological data and grids were designated by SN (station number) for this study purpose only to better represent ERA grid points in which daily rainfall and temperature of 1990–2021 were extracted and processed to analyze the annual and seasonal variability of climate in Ghibe III dam watershed.

The rainfall and temperature of meteorological station in Ghibe III Dam watershed used the various indices which help to measure the extreme events occurred (Table 3).

2.3. Data analysis methods

2.3.1. Observational data analysis methods (1990–2021)

The observational data for five stations namely Bele, Wolaita Sodo, Areka, Gena Bosa, and Gesuba were analyzed using Modified Mann-Kendall test in which sixteen climate extremes indices were analyzed in R4.2.2 software.

2.3.1.1. Methods for analyzing the spatial variability of precipitation and temperature. The methods used to analyze the spatio-temporal variability of rainfall and temperature were the number of days the extremes events occurred, mean, range, standard deviation and percentages. Rainfall and temperature extremes were computed using the RclimDex (version1) in R4.2.2 Software in Arc GIS environment. The sixteen rainfall and temperature extreme indices were selected for this study for analysis of spatial variability of rainfall and temperature for each of the five stations. The output of the extreme indices such as consecutive dry days, consecutive wet days, cool night, cool day, warm day, warm night, Number of very heavy precipitation days, Number of heavy precipitation days Max 1-day, warmest day, and warmest night all were spatially analyzed using interpolation in Arc GIS 10.3.

2.3.1.1.1. Areal distribution of rainfall and temperature. Areal value of rainfall or temperature was calculated using the following formula(equation (1)):

Table 2
Grids for ERA5 data in Ghibe III Dam watershed (1990–2021).

Station number (SN)	North Latitude (N)	East Longitude (E).	Elevation (m.a.s.l)
SN12	6.5	37.5	1317
SN21	6.75	37.25	820
SN22	6.75	37.5	1810
SN23	6.75	37.75	1873
SN31	7	37.25	2290
SN32	7	37.5	1238
SN33	7	37.75	1878
SN42	7.25	37.5	1989
SN43	7.25	37.75	2195

Table 3
Rainfall and Temperature extreme indices in Ghibe III Dam watershed (1990–2021).

Types of indices	Description	Explanations	Measurements
SDII	Simple daily intensity index	Annual total rainfall when (PRCP ≥1 mm) divided by the number of wet days	mm/day
CWD	Consecutive wet days	Maximum number of consecutive days with RF ≥ 1 mm	days
CDD	Consecutive dry days	Maximum number of consecutive days with RF < 1 mm	days
PRCPTOT	Annual total wet-day precipitation	Annual total rainfall from days ≥1 mm	mm
R95p	Very wet days	Annual total precipitation from the days with daily R F > 95th percentile	mm
R10mm	Number of heavy precipitation days	Annual counts of days when rainfall ≥10 mm	days
RX1day	Max 1-day precipitation amount	Annual maximum 1-day precipitation	mm
RX5day	Max-5-day precipitation amount	Annual maximum consecutive 5-day rainfall	mm
R20mm	Number of very heavy precipitation days	Annual counts of days when rainfall ≥20 mm	days
R99p	Extremely wet days	Annual total precipitation on the days when daily RF > 99th percentile	mm
TX90p	Warm days	Percentage of days when Tmax >90th percentile	days
TN90p	Warm nights	Percentage of days when Tmin >90th percentile	days
TX10p	Cool days	Percentage of days when Tmax <10th percentile	days
TN10p	Cool night	Percentage of days when Tmin <10th percentile	days
TXx	Warmest day	Annual maximum value of the daily max temperature	^{o}c
TNx	Warmest night	Annual maximum value of daily min temperature	^{o}c

$$P_a = \frac{\sum_{i=1}^{n} p_i A_i}{A} \quad (1)$$

where,Pa = average precipition,n = number of stations,p_i = precipitation at indvidual station, A_i = area of each polygon, and A is the total area of the watershed. First of all, area of each station was computed using the Theissen polygon. Thus, area of Bele station calculated was 46.08 km^2 (4608.43ha), Areka station 36.86 km^2 (3686.16 ha), Wolaita Sodo station was 47.7 km^2(4770.22ha), GenaBosa station was 103.86 km^2 (10385.98ha), Gessuba station was 19.17 km^2(1916.78ha) and their total area was 253.68 km^2 (25367.57ha). Each was multiplied by the area of the respective station and finally divided by the total area to get the area rainfall or temperature maximum and minimum.

2.3.1.2. Methods for analyzing the temporal variability of precipitation and temperature. The modified Mann-Kendall and Sens's slope test was used to detect the trend and magnitude in rainfall and temperature extremes. The temporal variability of temperature and rainfall was analyzed using the coefficient of variation and precipitation concentration index.

2.3.1.2.1. Coefficient of variation (CV). The coefficient of Variation (CV) is the relative indicator of variability within climate data set that indicates the size of standard deviation about its mean. It was used to analyze the spatiotemporal variability of annual, seasonal, and monthly rainfall as used by Achite et al [33]. The descriptive statistics such as mean, standard deviation, minimum value, maximum value,interquartile, first quartile, third quartile, interquartile range, and pseudo sigma were used according to Ferreira et al. [34] to compare the groups of rainfall and temperature data sets in current study area. A greater CV value indicates increased variability, and vice versa. Asfaw et al. [35] classified the degree of variability of rainfall events as low (CV < 20), moderate (20 < CV < 30), and high (CV > 30).

2.3.1.2.2. Precipitation concentration index (PCI). PCI is the statical derived concentration index used to quantify the relative distribution of rain fall over an area in given period of time as per Salhi et al. [36]. PCI examines rainfall variability (heterogeneity pattern) at various scales (annual or seasonal). The PCI values were computed as stated by Ngongondo et al. [37] and PCI of less than 10 indicates a regular monthly rainfall distribution, PCI of 11–20 indicates a high concentration, and PCI of 21 and beyond indicates a very high concentration. PCI as a variable compared by different statical methods such as mean, standard deviation and percentiles.

2.3.1.2.3. Modified Mann–kendall trend test and sen slope estimator. The modified Mann-Kendall was applied to analyze the temporal variability of rainfall and temperature and computed as proposed by Hamed & Rao [38]. The Modified Mann–Kendall tests have been applied with the aim of trend detection for monthly, seasonal, and annual time series data of the average temperature and rainfall as stated by Elzopy et al. [39]. The pros of modified Mann-Kendall test is that it allows to remove the serial correlation effect of meteorological variables by pre-whitening, variance correlation and over whitening and the cons of modified Mann-Kendall test is that for instance, pre-whitening which supposed to remove autocorrelation may remove a portion of trends, thus, this is a bone of contention among scientists and subject to criticism that has not been resolved yet as specified by Alashan [40].

2.3.1.2.4. Sen's slope estimator. Ademe et al. Ali Mohammed et al. [14,41] explained that linear trends are determined by Sen's slope estimator. However, this method requires the assumption of residual normality. Thus, Sen's Slope estimator is found to be a powerful tool to develop linear relationships having an advantage over the regression slope, in which raw data series errors and outliers do not have much effect. Pingale et al. [42] also described that in the non-parametric statistical tool, the magnitude of the trend that exists in the time series is estimated by Sen's slope estimator So, this study used the Sen slope to estimate the magnitude of the trends in the time series data in five selected stations.

2.3.2. Estimation of precipitation and temperature data by ERA 5 according to greenhouse gas emission scenarios

2.3.2.1. Bias correction of ERA5 reanalysis. Temperature and rainfall data extracted from ERA5 have been bias-corrected using meteorological data of Bele from 1990 to 2017. The monthly, seasonal, and annual time scales of ERA5 rainfall and temperature data were corrected. This is due to the difficulty of obtaining stations that can provide time series consistence and complete data in the area. Studies on the effects of climate change need reliable long-term data. Due to a lack of sufficient observed datasets, alternate proxy datasets are in high demand. As a result, ERA 5 data were used in this study as it appears to have the best performance in terms of capturing the many aspects of daily and annual rainfall with of course some limitations that they generally failed to spatially reflect long-term changes in annual rainfall according to Woldemariam et al. [43].

2.3.3. Estimation of precipitation and temperature data by climate models according to greenhouse gas emission scenarios

In this study, the CORDEX the dynamically downscaled models such as CCLM4, RACMO22T, RCA4, and REMO 2009 were used. The baseline for the present study is 1976–2005, and the projection period ranges from 2041 to 2100. Based on four regional circulation models (RCMs) and two representative concentration pathways (RCPs, 4.5 and 8.5), projected variations in rainfall and temperature were evaluated over the Gibe III Dam watershed.

2.3.3.1. Data quality control. The different data sets were used after ensuring their quality using various data quality control techniques. For instance, observed data were checked and missing values were corrected using the Markov chain model and inverse distance weighting method in excel. The data quality control was also performed using RclimDex in which potential outlies for rainfall and temperature were identified using interquartile range (IQR). The 25th and 75th percentiles were also used to identify outliers. The precipitation, maximum temperature (TXx), and daily temperature range (DTR) were checked. The missing values were corrected before its use. In all stations, duplicate dates, no large values, and no jumps were found. However, outliers in time series data were checked and represented graphically and numerically.

2.3.3.2. Testing the consistency of the rainfall data. Inconsistency may result from unreported shifting of the rain gauge in the gauging station. Double Mass Curve Analysis was used to adjust inconsistent data. In this study, the change in the regime of the curve of the inconsistency was adjusted using equation (2) (Fig. 2):

$$R_A = \frac{B_A}{A_o} x(R_O) \tag{2}$$

Where, R_A = adjusted Rainfall, R_O = Observed Rainfall, A_o = Slope of the graph at time R_O is observed, B_A = Slope of the graph to which records are adjusted.

2.3.3.3. Climate model performance evaluation. Historical (1976–2005) and (1999–2007) daily rainfall and temperature data of two stations (Bele and Gassachere) respectively were used.

2.3.3.4. Bias correcting RCM. Bias correction is usually required as climate models often provide biased representations of observed times series data due to systematic model errors caused by imperfect conceptualization, discretization, and spatial averaging within grid cells. As per Gleixner et al. and G. Worku et al. [31,44] bias correction was confirmed to be applied for compensating any tendency of overestimating or underestimating the mean of downscaled variables. In the CMhyd software, the average monthly precipitation was adjusted to match the average monthly precipitation for 30 years (1976–2005) for Bele and (1999–2007) for Gassachere stations.

The formula used for rainfall and temperature bias correction were presented (Equation(s 3) and (4)) respectively as follows:

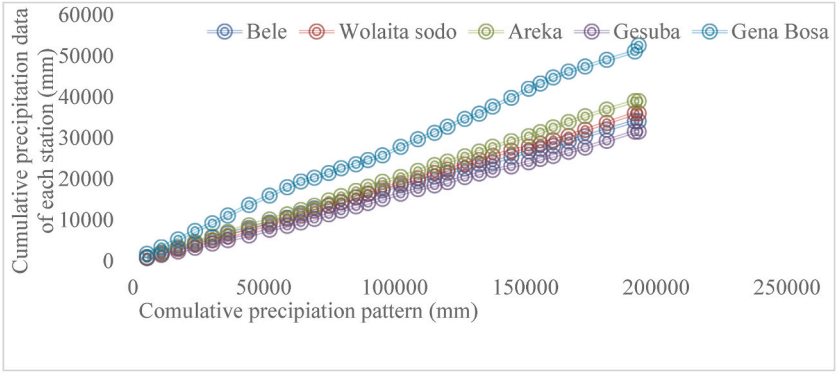

Fig. 2. Double mass curve of precipitation.

$$P_{bc} = p_p \frac{P_0}{P_r} \tag{3}$$

$$T_{bc} = T_p + T_o - T_r \tag{4}$$

where, P_{bc} = Bias corrected future rainfall amount in mm.

P_P= Predicted future rainfall amount in mm.

P_O = Mean of observed rainfall in mm.

P_r = Mean of computed historical rainfall during the observation period in mm.

T_{bc} = Bias corrected future temperature in 0c.

T_P=Predicted future temperature in 0c.

T_o = mean of observed temperature in 0c.

T_r = Mean of computed historical temperature during the observed period in 0c.

Distribution mapping, linear scaling, delta, and power transformation were the bias correction techniques that used to adjust historical simulations of rainfall and temperature of four RCMs to the values and distribution of observed rainfall. The performances of the regional climate models such as CCLM4, RACMO22T, RCA4 and REMO2009 were evaluated using BIAS, RMSE, and Correlation(r) (Equation 9-11). Besides, the BIAS evaluates the systematic error between the variables of the observed and simulated climates, with zero denoting good performance and values other than zero denoting departures from the observed data. The linear relationship between the average observed precipitation and the average RCM-simulated precipitation was shown by the correlation coefficient (r) as stated by Gado et al. [45]. The difference between RCM and observed rainfall is also measured by the RMSE. A lower RMSE value close to zero suggests better performance as per Li et al. [46].

$$BIAS = \frac{1}{n}\sum_{i=1}^{n}(Si - Oi) \tag{5}$$

$$RMSE = \sqrt{\frac{1}{n}\sum_{i=1}^{n}(Si - Oi)^2} \tag{6}$$

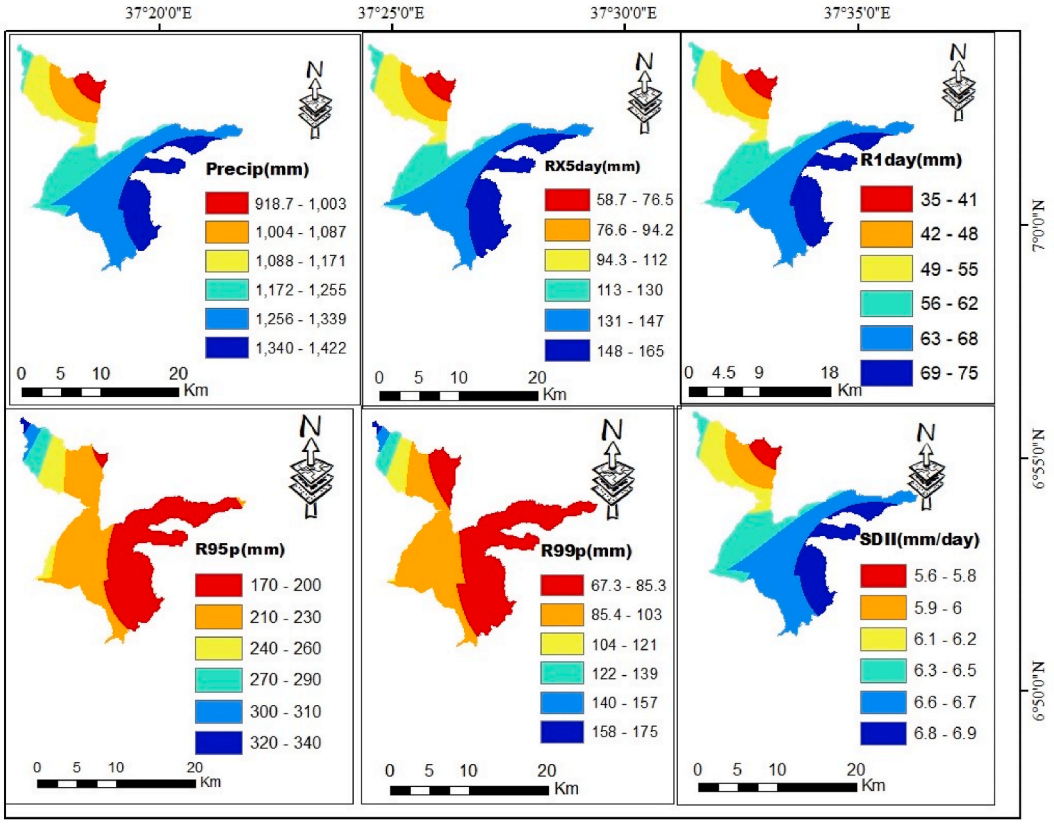

Fig. 3. Annual extreme rainfall intensity indices distribution in Ghibe III Dam watershed during 1990–2021.

$$r = \frac{\sum_{i=1}^{n}(Si - Sm)(Oi - Om)}{\sqrt{\sum_{i=1}^{n}(Si - Sm)^2}\sqrt{\sum_{i=1}^{n}(Oi - Om)^2}} \quad (7)$$

where S is the simulated value of the RCMs, O is the observed value of the climate variable, i refers to the simulated and observed pairs, n is the total number of the pairs and m refers to mean.

3. Results

3.1. Spatial and temporal variability of observational data during the period 1990–2021

3.1.1. Spatial variability

The spatial variability and trends in rainfall and temperature extremes were analyzed using different rainfall and temperature indices graphically and numerically. The rainfall intensity indices analysis indicates that PRCPTOT is in the range of 918.7 mm–1171 mm and found to be lowest at the central and extreme northeastern part of the Ghibe III Dam watershed and 1172–1422 mm at the highest part of the watershed. On the other hand, it was observed that RX1day, RX5day, and SDII were higher in the southern and eastern than in the northern and western parts of the watershed. Annual maximum 5-day precipitation (RX5day) ranges between 58.7 and 76.5 mm in northeastern and 148–165 mm in Southeastern parts. In terms of annual maximum 1-day precipitation (RX1day), the entire study area received low precipitation up to 55 mm. Similarly, very wet days (R95P) and annual total precipitation on the days when daily rainfall is greater than 99th percentile (R99p) were in range of low to high in the watershed. However, number of wet days index (SDII) was observed highest in the southeastern part than northeastern part (Fig. 3). The easternmost and northwestern parts of the study area experienced contrasting rainfall indices in the watershed.

Warm nights (TN90p) exhibited more days of warming during the night in the upper parts ranging from 7.5 to 75.98 days. The spatial distribution of annual warm days (TX90p) ranges from 11.34 to 57.1 days with higher heating in southern parts of the Gibe III Dam watershed. Only Gena Bosa, Gessuba, Bele, and Areka stations showed an increase in the frequency of cool nights (TN10p) and cold days (TX10p). The annual value of the hottest night minimum temperature, or TNxp, was 18.74 at Bele (Kindo Koisha District) and 19.73 °C at Gena Bosa (Loma Bosa District). The annual maximum temperature ranges from 34.24 °C to 34.75 °C on the warmest days (Txx). Tx10p with Tmin<10th percentile ranges from 2.79 to 8.4 days. The cool days (TX10p) range from 2.79 to 8.41 while cool night

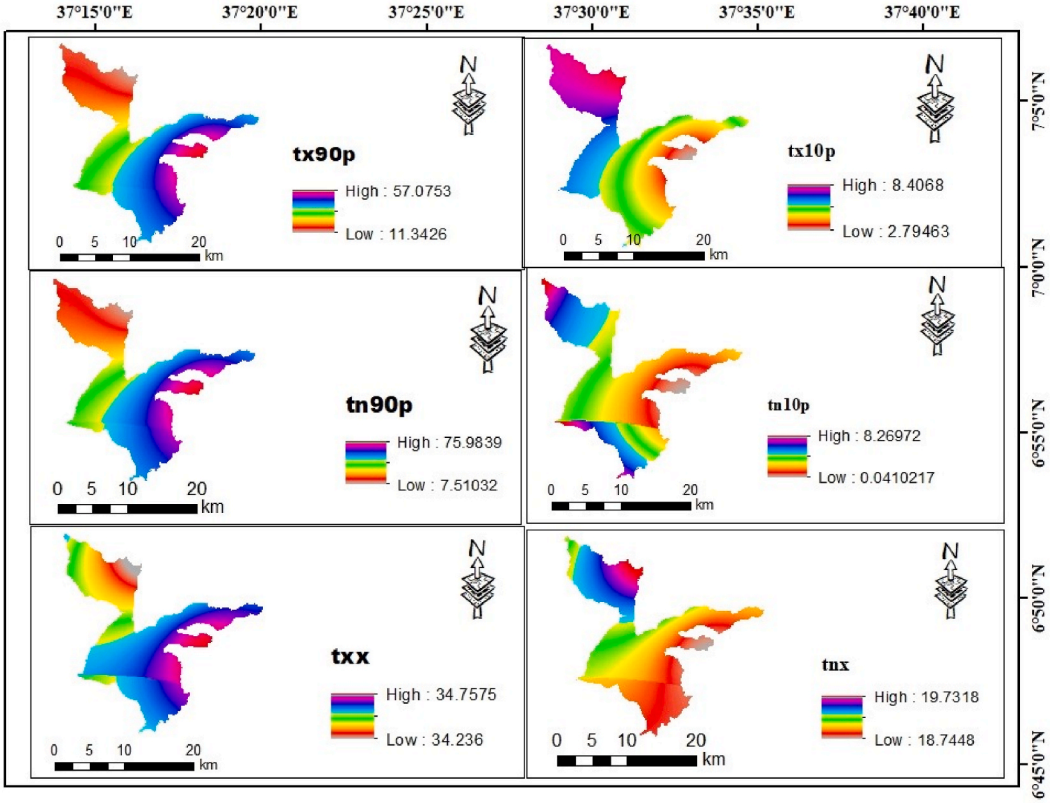

Fig. 4. Spatial distribution of temperature indices in Ghibe III Dam watershed during 1990–2021.

(10N10p) ranges from 0.04 to 8.26. But the opposite is true for cool nights (TN10p) which showed maximum cool nights in the Loma Bosa district and minimum cool nights in Koisha district. In terms of warm days (TX90p) or percentage of days when Tmax>90th percentile and warm nights (TN90p) or percentage of days when Tmin>90th percentile showed minimum and high in Loma and Kindo koisha districts respectively (Fig. 4). Temperature indices also varied in kind koisha district of which 75 % lies hot (local equivalent kola) agro ecology in low land and Loma Bosa district that its northern part, especially Chicho Haye *kebele*-smallest administrative unit lies in cool Woina Dega (temperate climate).

Spatial distribution of rainfall indices in terms of frequency showed that during 1990–2021, R20 and R10 were higher in the South East than North East parts of Ghibe III Dam watershed. However, CDD was lower in the southeast than Northeast in the watershed (Fig. 5). Thus, the rainfall extremes events varied spatially over the entire watershed. This showed that the occurrence of extreme events in the various parts of the watershed implying call for action to create resilient community in the river basin in Southern Ethiopia.

3.1.2. Temporal variability

Rainfall indices in terms of intensity using meteorological data.

SDII showed a significant increasing trend at a rate of 0.03 mm/day at Gessuba and Wolaita Sodo stations at ($P < 0.05$) while showing a decreasing trend at Bele station with the rate of change of −0.09 at 5 %. Similarly, SDII showed a decreasing trend with rate of change of −0.01 but insignificant at Areka station. RX5 day showed an increasing trend for all stations except Wolaita Sodo. Rx1day showed an upward trend($P < 0.05$) at the rate of 0.4 mm day for Wolaita Sodo and it showed a decreasing trend at rate of −0.39 for Bele station. In Wolaita Sodo station, at a rate of 1.95 mm/day and for Gena Bosa at a rate of 2.33 mm/day, R99p exhibited an increasing trend ($P < 0.05$). The yearly total wet-day precipitation (PRCPTOT) exhibited decreasing trend and insignificant at Gena Bosa. However, R95p showed decreasing significant trend for Bele and Areka (Table 4). The rainfall extremes indices showed the increasing and decreasing trends at different stations with various rate of change indicating variability in rainfall.

3.1.2.1. Rainfall indices in terms of frequency. Consecutive Dry Days (CDD) exhibited an upward trend for all stations but insignificant except for Gena Bosa station. Consecutive Wet Days (CWD) showed an upward significant trend at Areka and Gessuba while downward significant trend at Gena Bosa. R20mm exhibited an increasing significant trend at Wolaita Sodo and Gesuba while decreasing insignificant trend at Bele and Areka. R10mm showed a decreasing and non-significant trend for all station except Gesuba (Table 5).

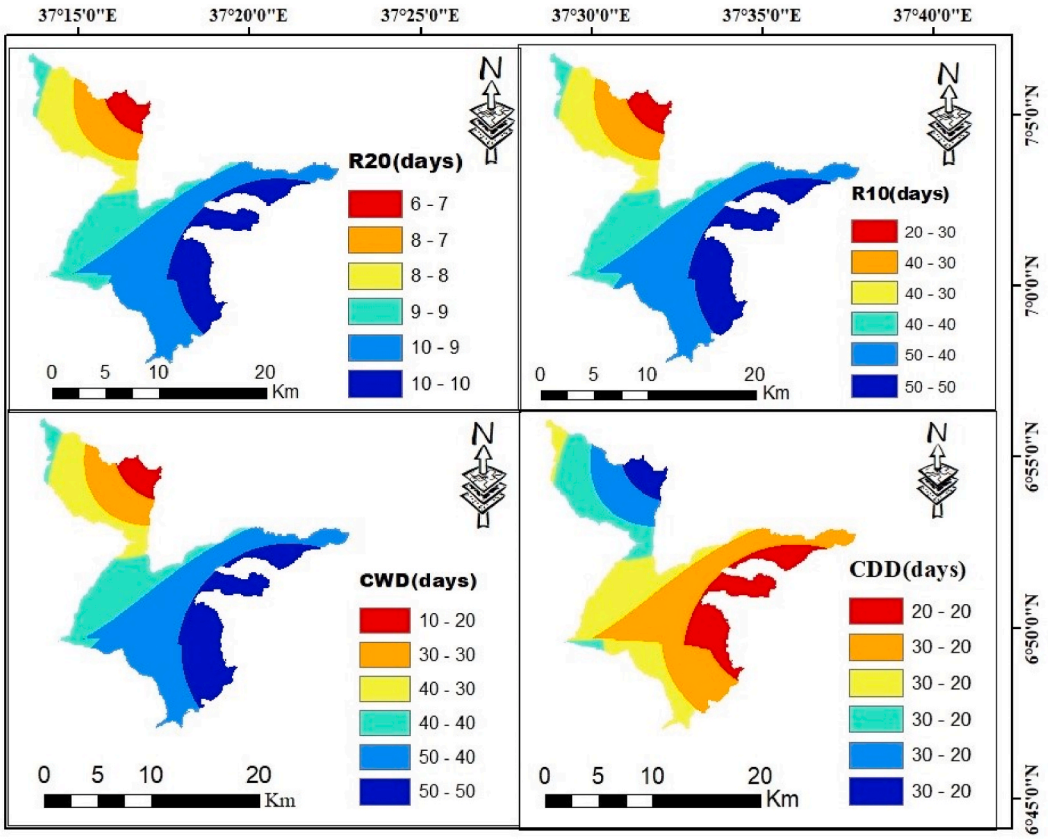

Fig. 5. Spatial distribution of rainfall indices in terms of frequency in Ghibe III Dam watershed during 1990–2021.

Table 4
Modified Mann-Kendall trend test statistics of rainfall intensity in Ghibe III Dam watershed (1990–2021).

Indices	Trend Tests	Bele	Wolaita	Areka	Gena Bosa	Gesuba
SDII	Zc	−5.65	2.16	−1.27	0.15	3.08
	p-value	0.00	0.03	0.20	0.88	0.00
	SS	−0.09	0.03	−0.01	0.00	0.03
RX5 day	Zc	2.39	1.37	2.28	2.25	3.66
	p-value	0.02	0.17	0.02	0.02	0.00
	SS	0.45	0.54	0.79	0.82	1.05
RX1 day	Zc	−2.85	2.14	−0.39	2.77	0.7
	p-value	0.00	0.03	0.70	0.01	0.48
	SS	−0.39	0.4	−0.03	0.57	0.13
R99p	Zc	−0.75	2.16	−0.84	2.37	1.1
p-value	p-value	0.45	0.03	0.4	0.02	0.27
	SS	0.00	1.95	−0.13	2.33	0.00
R95p	Zc	−2.54	2.19	−2.00	1.64	1.72
p-value	p-value	0.01	0.03	0.05	0.10	0.09
	SS	−2.22	3.61	−3.53	5.83	2.29
PRECPTOT	Zc	0.86	2.31	2.17	−0.93	2.41
	p-value	0.39	0.02	0.03	0.35	0.02
	SS	4.32	7.66	6.11	−5.81	7.27

Zc = Corrected Z; p-value = new p-value; SS = Sens's slope.

Table 5
Modified Mann-Kendall trend statistics of frequency indices in Ghibe III Dam watershed (1990–2021).

Indices	Trend Tests	Bele	Wolaita	Areka	Gena Bosa	Gesuba
CDD	Zc	0.59	1.9	0.71	4.69	1.44
	p-value	0.56	0.06	0.48	0.00	0.15
	SS	0.12	0.31	0.08	0.32	0.24
CWD	Zc	1.63	1.71	5.31	−2.09	3.02
	p-value	0.1	0.09	0.00	0.04	0.00
	SS	0.18	0.17	0.78	−0.77	0.24
R20mm	Zc	−4.07	2.62	−2.31	1.46	3
	p-value	0.00	0.01	0.02	0.14	0.00
	SS	−0.22	0.1	−0.11	0.13	0.09
R10mm	Zc	−0.05	1.77	1.01	−0.64	2.69
	p-value	0.96	0.08	0.31	0.52	0.01
	SS	0.00	0.23	0.14	−0.2	0.28

Zc = Corrected Z; p-value = new p-value; SS = Sens's slope

Table 6
Modified Mann-Kendal trend statistics of temperature in Ghibe III Dam watershed (1990–2021).

Indices Trend Tests		Bele	Wolaita	Areka	Gena Bosa	Gesuba
TX90p	Zc	2.10	5.65	−0.63	1.80	−3.47
	p-value	0.04	0.00	0.53	0.07	0.00
	SS	0.30	0.32	−0.03	0.18	−0.37
TN90p	Zc	1.91	1.76	−2.64	4.60	−3.46
	p-value	0.06	0.08	0.01	0.00	0.00
	SS	0.07	0.15	−0.31	0.31	−0.3
TX10p	Zc	−2.98	−1.03	−0.62	−3.81	−0.01
	p-value	0.00	0.3	0.53	0.00	0.99
	SS	−0.18	−0.2	−0.05	−0.18	0.00
TN10p	Zc	0.73	0.37	4.06	−3.75	1.41
	p-value	0.47	0.71	0.00	0.00	0.16
	SS	0.07	0.01	0.40	−0.13	0.03
TXX	Zc	3.4	4.31	2.22	3.61	1.09
	p-value	0.00	0.00	0.03	0.00	0.27
	SS	0.11	0.07	0.02	0.09	0.02
TNX	Zc	5.41	5.34	−1.97	5.01	−3.31
	p-value	0.00	0.00	0.05	0.00	0.00
	SS	0.15	0.09	−0.02	0.03	−0.05

Zc = Corrected Z; p-value = new p-value; SS = Sens's slope

The areal average temperature maximum and minimum was 26.37^{0}c and 13.81^{0}c respectively with average precipitation of 1446.92 mm over the entire watershed.

3.1.2.2. Temperature indices trend analysis. The result indicated that rising annual warm days (TX90p) showed increasing significant trend at Bele and Wolaita Sodo while showing a decreasing significant trend at Gesuba at $P < 0.05$. The Warm nights (TN90p) showed increasing significant trend at Gena Bosa while showing decreasing significant trend at ($P < 0.05$) for Areka and Gesuba. The TNx and TXx showed increasing trends for Bele, Wolaita Sodo and Gena Bosa. At Gesuba station, TX90p, TN90p and TNX showed a decreasing and significant trend. At Gena Bosa station, TN90p, TXX and TNX showed an increasing significant trend at ($P < 0.05$). Contrarily, TX10p and TN10p showed a decreasing significant trend at a 5 % significant level (Table 6). The temperature indices showed the overall warming trend over the Ghibe III Dam watershed for 1990 to 2021.

3.2. Estimation of precipitation and temperature data by ERA5

3.2.1. Performance evaluation of ERA5 precipitation/Temperature

The observed and simulated ERA 5 data showed a significant association with R^2 values ranging from 0.91 to 0.99, while the RMSE ranges from 0.01 to 0.17. The SN22 value is very close to zero, which indicates greater performance agreement between the observed and the simulated data. A bias of 0.83 for SN21 indicates that ERA 5 and measured data have a good level of agreement (Table 7). ERA5 achieves a moderate positive bias worldwide. It is a valid alternative for situations in which satellite-based data are missing. However, Urraca et al. [47] stated that ERA5 is sometimes underestimating the values and shows negative bias. ERA data can be even used for RCM model validation in the absence of a meteorological station. Thus, it is important to use ERA 5 data for the analysis of climate variability according to Mutayoba & Kashaigili [48]. The mean, standard deviation, and median of the ensemble average of ERA 5 data are close to those from the ERA-interim reanalysis Mutayoba & Kashaigili [48]. From the analysis, it can be concluded that the ensemble mean performs better compared to the individual RCMs.

The mean annual precipitation concentration index revealed that Ghibe III Dam watershed has 67.74 % irregular and 19.35 % highly erratic rainfall distribution. However, between 1990 and 2021, the area experienced 12 % increase in moderate rainfall (Table 8). The agricultural sector of the community, which is reliant on rainfall, is threatened by spatio-temporally unpredictability, unequal and irregular distribution of precipitation in the watershed. The PCI result showed irregular and strong erratic rainfall distribution (87 %) in Ghibe III dam watershed.

SN22, SN32, and SN33 displayed an increasing trend that was statistically significant at the 95 % confidence level, with slope values of 3.34, 3.5, and 7.1, respectively. Over the Watershed, the areas represented by SNs 12, 21, 31, and 43 showed a declining trend, but insignificant whereas SN23 and SN42 showed an insignificant increasing trend in rainfall (Table 9 and Fig. 6). This result indicates that there are upward and downward trends in the rainfall.

All temperature trend analyses using ERA5 data demonstrated an increasing trend with ($P < 0.05$) and a positive slope (Fig. 7), indicating that temperature in the Gibe III Dam watershed has been rising periodically and will likely continue to do so in the future.

The mean annual rainfall coefficient of variation (CV) ranges from 33 % to 79.8 %. The variability of rainfall is higher in winter (DJF) than in summer (JJA), spring (MAM), and autumn (SON) seasons. For instance, Summer (June–August) has CV ranging from 38 to 64 %, Winter (December–February) has CV of 72.4–99.3, Spring (March–May) has CV of 30–90 % and Autumn has CV of 76–86 %. The annual and seasonal rainfall varied in the watershed from 1990 to 2021. However, seasonal variability was higher than annual variability. Thus, Winter season (DJF) known as locally Bega has higher variability than other seasons in the study area. The mean annual rainfall across the 9 stations designated by SN ranged from 454 mm (SN32) to 1393 mm (SN12) (Table 10). All of the stations showed higher variations in seasonal and annual rainfall (CV%>30). In most of the stations the PCI value is between 10 and 20 % showing the seasonality in rainfall distribution Both CV and PCI exhibited variability in rainfall distribution in the study area.

The highest mean rainfall was 169.65 mm in April, 125.07 mm in May, 121.45 mm in July, and 122.98 mm in August. The smallest mean rainfall record occurred in January (31.56 mm), whereas the highest mean monthly rainfall occurred in April (169.65) followed by May(125.04 mm) (Fig. 8). The rainfall has a bimodal pattern in which the highest amount of rainfall received in spring season followed by summer season.

The mean monthly temperature distribution based on ERA5 also showed variability. Temperature showed fluctuating pattern through the entire watershed over the 1990–2021(Fig. 9).

The annual temperature coefficient of variation ranges from 1.7 % to 2 % whereas the seasonal CV ranges from 3.1 % to 3.9 % in Summer, 3 %–3.7 % in Winter, 3 % to 3.9 % in Spring and 0 % to 18.4 % in Autumn (Meher) (Table 11). Similar to rainfall, temperature exhibited higher seasonal variability than annual variability.

Table 7
Performance evaluation of ERA5 reanalysis in Ghibe III Dam watershed (1990–2021).

Station Number	RMSE	R^2	Bias
SN21	0.17	0.98	0.83
SN22	0.01	0.99	−0.75
SN31	0.1	0.93	−89
SN32	0.13	0.91	−115

Table 8
Precipitation concentration index in Ghibe III Dam watershed based on ERA 5 (1990–2021).

PCI	Categories	Years	%
<10	Uniform rainfall distribution	0	0
10 to 15	Moderate rainfall distribution	4	12
16–20	An irregular rainfall distribution	21	67.74
>20	Strong erratic rainfall distribution	6	19.35

Table 9
Modified Mann Kendall trend statistics of rainfall based on ERA reanalysis (1990–2021).

Station	Zc	p-value	SS
SN12	−0.40	0.69	−1.27
SN21	−0.21	0.83	−0.36
SN22	2.35	0.02	3.34
SN23	1.3	0.2	4.0
SN31	−0.43	0.67	−0.48
SN32	3.2	0.00	3.5
SN33	2.3	0.02	7.1
SN42	1.0	0.3	1.74
SN43	−0.8	0.4	−2.72

Zc = Corrected Z; p-value = new p-value; SS = Sens's slope.

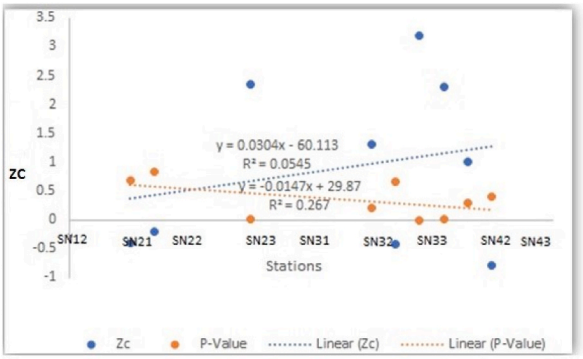

Fig. 6. Modified Mann kendall trend statistics of rainfall based on ERA reanalysis (1990–2021).

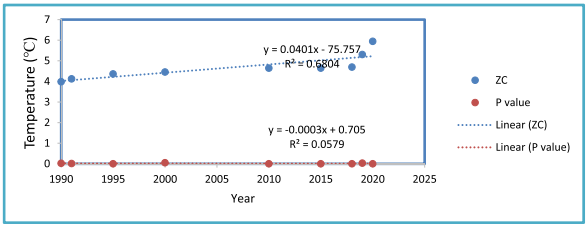

Fig. 7. Modified Mann-Kendall test results of Temperature based on ERA reanalysis (1990–2021).

3.3. Estimation of precipitation and temperature data by climate models

Compared to individual regional climate models (RCM), the ensemble mean of RCMs exhibits a greater correlation with observed annual rainfall data. For instance, the ensembled RCM performed (r = 0.6 %) better than the individuals RCM such as CCLM(r = −0.02), RACMO(r = −0.01) and RAC4(r = 0.09). Remo (r = −0.03) and RACM022T (r = −0.02 %) showed a linear relationship between actual and predicted rainfall amounts This is in line with Demissie and Sime [49] in which ensemble mean for RCMs ranged from −0.02 up to 6.73 at varying stations. Additionally, the ensemble mean low coefficient of variation (CV = 11.5 %) in relation to the observed rainfall indicated that observed rainfall and ensemble mean were closely related. The rainfall in the watershed is not accurately represented by all models, some models slightly underestimate and others overestimate the observed rainfall (Table 12).

Table 10
Comparing annual &seasonal rainfall(mm),CV(%)& PCI for stations in &around Ghibe III dam area using ERA 5(1990–2021).

SN	Mean annual RF(mm)	CV (%)	Summer (JJA) RF(mm)	CV (%)	Winter (DJF)RF (mm)	CV (%)	Spring (MAM)	CV (%)	Autumn (SON) RF (mm)	CV (%)	PCI
SN12	1393	37	443	57	132	83	510	89	308	79	19.4
SN21	1094.8	36.5	360.7	56.5	89.7	82.5	400	87.2	244.3	78	19.6
SN22	1032	34	332	52	93	88	367	83	240	79	18.9
SN23	927	38	259	47	162	81	358	90	148	86	19.2
SN31	579	40	181	47.2	62	99.3	235	87.5	101	76	19.1
SN32	454	36.2	140.4	42.1	48.1	95.78	48	30	84.2	79	19.3
SN33	1194	33	338	38	193	86	469	77	192	79	18.5
SN42	542	79.8	159.5	64	39.39	97.35	186.5	89	88.5	84	23.5
SN43	1250	52.9	378.1	55.2	104	72.4	452	78.9	222	78	21.5

DJF = December, January,February; MAM = March, April,May; JJA = June, July,August,SON=September, October & November.

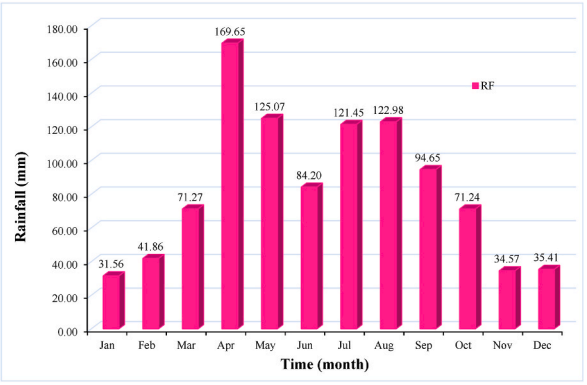

Fig. 8. Mean monthly rainfall distribution based on ERA5 in Ghibe III Dam watershed (1990–2021).

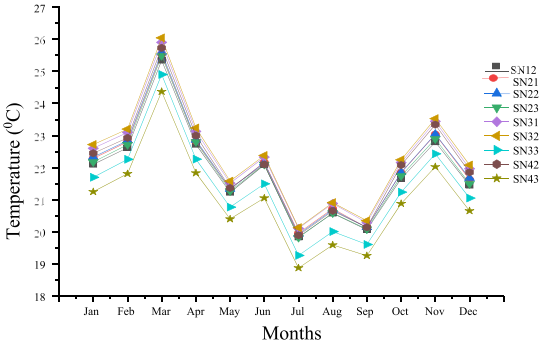

Fig. 9. Mean monthly temperature distribution based on ERA5(1990–2021).

The REMO2009 performs the best (PBias = −9.81 %), and the group mean performs the worst (PBias = −19.65 %). The high bias (PBias = −44.99 %) indicates that the RCM rainfall amount considerably differs from the observed rainfall amount. Additionally, MPI-CCLM4 performs poorly (RMSE = 19.98 mm year-1), while the ensemble mean performed the best (RMSE = 6.73 mm year-1). All models perform the worst for Root mean square. Due to better performance, the ensemble mean of climate models has been used to study climate change projection. The ensemble mean of individual regional climate models has the best performance based on performance evaluation criteria and has ability to capture the annual observed rainfall amount relative to individual climate models.

Climate change produces variability in its elements such as rainfall and temperature, Thus, understanding the climate change is vital for the analysis of the variability of rainfall and temperature extremes. This study showed high (CV = 20.65 %) in CCLM for two representative concentrations path (4.5& 8.5), and extremely high variability of rainfall (CV = 93.49 %) in RACMO for RCP 4.5. Under the two scenarios, rainfall would generally decline throughout the watershed. Under the RCP 4.5 and RCP 8.5 scenarios in CLLM, the mean annual rainfall for the historical period (1976–2005) was 1061.1 mm. However, the same model's Mid Term (1941–2070) RCP

Table 11
Mean annual & seasonal variability of temperature in Ghibe III Dam watershed (1990–2021).

SN	annual average (T_C^O)	CV (%)	Summer (T_C^O)	CV (%)	Winter (T_C^O)	CV (%)	Spring) (T_C^O)	CV (%)	Autumn (T_C^O)	CV (%)
12	21.9	1.7	20.9	3.3	22.1	3.0	23.1	3.0	21.5	1.5
21	22.1	1.7	21.0	3.1	22.3	3.2	23.2	3.1	21.7	1.5
22	22.1	1.7	21.0	3.3	22.3	3.3	23.3	3.3	21.0	18.3
23	22.0	1.8	20.9	3.6	22.1	3.2	23.2	3.3	20.9	18.3
31	22.3	1.7	21.1	3.5	22.6	3.5	23.5	3.5	21.3	18.3
32	22.4	1.8	21.2	3.7	22.7	3.6	23.6	3.7	21.3	18.4
33	21.4	2.0	20.3	3.8	21.7	3.6	22.6	3.8	20.4	18.4
42	22.2	1.8	20.9	3.9	22.4	3.6	23.4	3.9	0.0	0.0
43	21.0	2.0	19.9	3.9	21.2	3.7	22.2	3.9	20.1	18.4

Table 12
Performance of precipitation of RCP for overlapping periods(1976–2005) in Ghibe III Dam watershed.

Data Type	Annual Rainfall (mm)	PBias (%)	RMSE (mmyear-1)	Correlation (−)	CV (%)
Observed	1043.62	-	-	-	30.69
MPI-CCLM4	574.06	−44.99	19.98	−0.15	20.49
RACMO22T	970.8	−12.66	7.16	−0.02	15.42
RAC4	927.9	−11.91	7.05	0.09	28.63
REMO 2009	952.63	−9.81	6.28	−0.03	21.33
Ensemble mean	856.38	−19.65	6.73	0.6	11.51

4.5 and RCP 8.5 scenarios showed increase in rainfall to 1080.23 mm and 1087.4 mm, respectively. However, under the RCP 4.5 and RCP 8.5 scenarios, it indicated a decrease in the future time, which is 835.8 mm and 776.96 mm, respectively. All models (CLLM, RACMO, RAC4, and REMO2009) revealed a declining trend in mean annual rainfall from 1976 to 2100. Rainfall showed higher variability as compared to temperature (Table 13). The rainfall showed a declining trend while temperature showed increasing trends from the base period to the long term in the Ghibe III Dam watershed.

The maximum mean temperature of the base period in RACMO was 22.46 °C.Under two representative scenarios, the maximum mean temperature would increase to 23.1 °C and 23.7 °C in the mid-term period and 23.63 °C and 24.8 °C for the long term, respectively. The coefficients of variation for these scenarios are 2.4 %, 2.74 %, 2.9 %, 2.87 %, and 2.75 %.

The minimum temperature was 7.7 °C for the base period, and it would be 9.34 °C and 10.1 °C for the mid-term under 4.5 and 8.5 scenarios respectively. Similarly, the minimum temperature was 15.87 °C and 12.76C for the long-term under RCP4.5 and 8.5 in RACMO.

The minimum temperature during the base period in RACMO was 7.70 °C and it is expected to increase to 9.34 °C and 10.10 °C in the mid-term period under two representative scenarios. Similarly, the minimum temperature is expected to be 15.87 °C and 12.76 °C for the long-term under RCP4.5 and 8.5 in RACMO, respectively. Temperatures for RAC4 and REMO showed a rising and falling trend (Table 14). In terms of minimum temperature, the area showed less variability (CV = 2.38) for the base period and high variability (CV = 20.1) in RACMO (Table 14). Thus, based on the RCM output localized to the study area, using coordinates of stations of Bele and Gassachere, the study showed that temperature showed an increasing trend over the years showing interannual and interdecadal variability.

4. Discussion

The discussion was subdivided into two distinct parts: the spatial and temporal variability of the observed data and the spatial and temporal variability of the data estimated by climate models.

4.1. The spatial and temporal variability of the observed data

Spatial distribution of rainfall indices in terms of frequency showed that during 1990–2021, R20 and R10 were higher in the South East than North East parts of the Ghibe III Dam watershed. However, CDD was lower in the southeast than Northeast in the watershed.

The result of the trend of rainfall extremes indices at five stations showed generally decreasing and increasing trends in rainfall and temperature extremes over the watershed. For instance, Consecutive Dry Days (CDD) exhibited an upward trend for all stations but insignificant except Gena Bosa. Consecutive Wet Days (CWD) showed an upward significant trend at Areka and Gessuba while downward significant trend at Gena Bosa. R20mm exhibited an increasing significant trend at Wolaita Sodo and Gesuba while decreasing insignificant trend at Bele and Areka. R10mm showed a decreasing and non-significant trend for all station except Gesuba. The annual warm days (TX90p) showed increasing significant trend at Bele and Wolaita Sodo while showing a decreasing significant trend at Gesuba. The Warm nights (TN90p) showed increasing significant trend at Gena Bosa while showing decreasing trend at Areka and Gesuba.

The TNx and TXx showed increasing trends for Bele, Wolaita Sodo and Gena Bosa. At Gesuba station, TX90p, TN90p, and TNX

Table 13
% of change, SD, Mean &CV of rainfall of Bele station in Ghibe III Dam watershed.

Periods/Terms	RCM	RCP	% of change	SD	Mean	CV (%)
Base period (1976–2005)	CCLM	4.5		219.15	1061.1	20.65
		8.5		219.15	1061.1	20.65
Mid Term (1941–2070)		4.5	1.8	325	1080.23	30.18
		8.5	2.47	581.98	1087.4	53.57
Long term (2071–2100)		4.5	−21.22	277.18	835.8	33.16
		8.5	−26.77	280.93	776.96	36.15
Base period (1976–2005)	RACMO	4.5		481.92	1023.51	47.08
		8.5		481.92	1023.51	47.08
Mid Term (1941–2070)		4.5	34.2	311.86	1172.58	26.59
		8.5	8	520.36	1106.38	47.03
Long term (2071–2100)		4.5	42	498.46	533.55	93.49
		8.5	2.55	479.13	1049.71	45.64
Base period (1976–2005)	RAC4	4.5		338.32	1096.86	30.84
		8.5		338.32	1096.86	30.84
Mid Term (2041–2070)		4.5	−2.7	471.22	1066.94	44.165
		8.5	−10.68	539.88	979.69	55.12
		4.5	0.59	613	110.35	55.56
Long term (2071–2100)		8.5	−13.32	569.27	950.8	59.87
Base period (1976–2005)	REMO2009	4.5		434.8	1018.62	42.68
		8.5		434.8	1018.62	56.36
Mid Term (1941–2070)		4.5		589.15	1045.19	56.36
		8.5	−8.9	526.8	927.17	56.82
Long term (2071–2100)		4.5	−0.08	573.9	1017.7	56.39
		8.5	−75.4	44.89	804.95	55.89

RCP=Representative concentration path, SD= Standard deviation, CV= Coefficient of variability.

showed a decreasing significant trend. At Gena Bosa station, TN90P, TXX and TNX showed an increasing significant trend at ($P < 0.05$). Contrarily, TX10p and TN10P showed a decreasing significant trend at a 5 % significant level. This result is in line with Benson et al. [50] who found a decrease in cool nights and cool days (TN10P, TX10P), and an increasing trend in warm nights and days (TN90P, TX90P). Likewise, it is inconsistent with Chang'a et al. [44], who reported a decrease of 7.64 % and 10 %, respectively, in the number of cold days and nights. Very wet days(R95p) showed a significant increasing trend at a rate of 3.6 mm/day for wolaita Sodo ($P < 0.05$). This is in line with Likinaw et al. [51] who reported that R95p (2.21 mm/year) and R99p (0.78 mm/year) had statistically significant increasing trends in Lay Gayint at $p < 0.05$ in Tach Gayint in North West Ethiopia.

On the contrary, R95p showed a decreasing significant trend for Bele and Areka. However, R95p showed a decreasing significant trend for Bele and Areka. This is incongruent with Wubaye et al. [11] in which rainfall showed a downward significant trend in many of the gauge stations. The temperature indices showed the overall warming trend over the Ghibe III Dam watershed. This is consistent with Ali et al. [52] the warming trend of the annual and seasonal maximum and minimum temperature extreme indices observed in Ethiopia's Upper Blue Nile. The areal average temperature maximum and minimum was 26.37°Cand 13.81 °C respectively with average precipitation of 1446.92 mm over the entire watershed.

The spatial distribution of annual warm days (TX90p) ranges from 11.34 to 57.1 days with higher heating in southern parts of the Gibe III Dam watershed. Temperature indices also varied in kind koisha district of which 75 % lies hot (local equivalent kola) agro ecology in low land and Loma Bosa district that its northern part, Chicho Haye kebele-smallest administrative unit lies in cool Woina Dega (temperate climate).

4.2. Spatial and temporal variability of data estimated by climate models

The highest mean record of rainfall was 169.65 mm in April, 125.07 mm in May, 121.45 mm in July, and 122.98 mm in August. The smallest mean rainfall record was 31.56 mm in January, 34.57 mm in November, 35.41 mm in December, and 41.86 mm in February. This is in line with Chiaravalloti et al. [53], in which rainfall on a seasonal scale, especially in the winter season, showed a declining trend. In Ethiopia, the winter season includes December, January, and February, when the lowest mean rainfall was observed.

The reason behind the highest rainfall record in April, ending up in August, was that the area receives rainfall during the spring and summer seasons. The temperature also showed variability across the entire watershed. Winter season (DJF) now, as locally Bega in Ethiopia has higher variability than other seasons in the study area, The mean annual precipitation concentration index exhibited 67.74 % irregular rainfall distribution and 19.35 % highly erratic rainfall distribution. This is incongruent with Arega et al. [54]in which high and irregular concentration of rainfall was observed in the eastern highlands of Ethiopia.

Based on ERA reanalysis, it was found that the annual and seasonal rainfall varied across the watershed from 1990 to 2021, having a variety of effects in the area. However, seasonal variability was higher than annual variability. This is in line with Bayable et al. [55], in which seasonal rainfall showed higher variability than annual rainfall. This has implications for rain-fed agriculture in Ethiopia. Similar result was also reported by Asfaw et al. [35] in north central Ethiopia.

The findings of the current study showed high variability (CV = 20.65 %) in CCLM under RCP 4.5 and 8.5 and extremely high

Table 14
% of change, SD, Mean & CV of Tmax &Tmin for Bele station in Ghibe III Dam watershed.

Tmax (^{O}c)	RCM	RCP	% of change	SD	Mean	CV (%)
Base period	RACMO	4.5		0.5	22.46	2.38
		8.5		0.5	22.46	2.38
Mid term		4.5	3.81	0.6	23.31	2.74
		8.5	5.5	0.7	23.7	2.9
Long term		4.5	5.16	0.7	23.63	2.87
		8.5	10.6	0.7	24.8	2.75
Tmin(^{o}c)						
Base period		4.5		1.6	7.7	20.1
		8.5		1.6	7.7	20.1
Mid term		4.5	20.6	1.7	9.34	18.16
		8.5	29.76	1.7	10.08	17.1
Long term		4.5	27.9	1.6	15.87	9.77
		8.5	57.84	1.4	12.76	11.63
Tmax(^{o}c)	RAC4					
Base period		4.5		0.57	22.58	2.54
		8.5		0.56	22.53	2.37
Mid term		4.5	4.26	0.75	23.54	3.2
		8.5	6.8	0.76	11.79	6.45
Long term		4.5	6.3	0.79	24	3.3
		8.5	11.67	0.91	25.16	3.622
Tmin(^{o}c)						
Base period		4.5		1.5	17.89	19.78
		8.5		1.5	17.89	19.78
Mid term		4.5	20.6	1.7	9.34	18.16
		8.5	29.76	1.73	10.08	17.1
Long term		4.5	27.9	1.55	15.87	9.77
		8.5	57.84	1.4	12.26	11.63
Tmax(^{o}c)	REMO					
Base period		4.5		0.5	22.6	2.4
		8.5		0.5	22.6	2.4
Mid term		4.5	4.8	0.6	23.6	2.59
		8.5	7.7	0.7	24.2	2.9
Long term		4.5	6.5	0.8	24	3.2
		8.5	12.3	0.9	25.3	3.4
Tmin(^{o}c)						
Base period		4.5		1.5	7.9	19.3
		8.5		1.5	7.9	19.3
Mid term		4.5	23.31	1.5	9.75	15.65
		8.5	47.7	1.5	11.7	12.45
Long term		4.5	30.99	1.5	10.4	14.38
		8.5	58.9	1.5	12.6	11.89

variability of rainfall (CV = 93.49 %) in RACMO under RCP 4.5. The mean annual rainfall showed a decreasing trend from 1976 to 2100 in the watershed in all models used in the present study (CLLM, RACMO, RAC4, and REMO 2009). This is in line with Nannawo et al. [56], in which rainfall showed a declining trend under the RCP 8.5 scenario in the Bilate basin in Ethiopia. In contrast to this, Mugo et al. [57] showed a positive significant trend at 5 % under RCP4.5 and 8.5 scenarios during March, April,May,October, November and December seasons.

A study by Teshome et al. [58] revealed that the mean annual minimum and maximum temperature is expected to rise in the Eastern and Western Hararghe Zones in Ethiopia by 0.34 °C and 2.52 °C for 2030 and 0.41 °C and 4.15 °C for 2050 under RCP4.5 and RCP8.5, respectively. The current study was similar with Ayalew [59] reported that the average annual precipitation varies between −37.3 % to 33.1 %, and −38.2 %, to 61.2 %, for RCP 4.5 and RCP 8.5, respectively. The anticipated declines in mean seasonal rainfall changes for the Bega and Belg seasons range from −69.6 % to 88.4 % and from −60.6 % to 15.2 % for RCP 4.5 and RCP 8.5, respectively. The average periodic precipitation considered for the Kiremt season will vary from −12.1 % to 1.33 %. Belg, Kiremt, and Bega seasons will likely see a 28.2 %, 12.2 %, and 22.6 % drop in mean seasonal precipitation, respectively in Hare Catchment of Ethiopia.

Similar results were also reported by Geleta et al. [60] in which monthly maximum temperature increase is projected to be 1.41 °C and 2.82 °C by 2050 and 2080, respectively. In contrast, the monthly minimum temperature increase is projected to reach +3.2 °C in 2080. The overall seasonal multi-model ensemble average shows an increment in maximum temperature by +1.1 °C and +1.9 °C in 2050 and 2080, with the highest change in the winter, followed by spring, summer, and autumn. Similarly, the future minimum temperature is projected to increase across all seasons by 2080, with increases ranging from 0.4 °C (2030s) to 3.2 °C(2080s) in South West Ethiopia.

Climate change produces variability in local climate conditions all spatial variability in rainfall and temperature is happening the changes in regional and global weather system. Besides, there spatial variability is created due to altitude for instance, there is difference in elevation of area such Bele(1250 m),Arek(1752 m), Gena Bosa(1741 m), Wolaita Sodo(1854 m), and Gesuba(1552 m). At

higher parts of the watershed, the air is less thick having less impact whereas at lower altitudes the air is more thick having more impact thus, spatially, depending on the altitude the rainfall and temperature varies. Thus, at lower parts in the Ghibe III Dam watershed, there is higher spatial variability than higher parts so lower parts are more vulnerable than higher parts. The higher or upper parts are more stable and produce annual and perennial crops so which is relatively conducive for crop production in the current study area. This is in line with Eeckman et al. [61] who reported that altitude affects the spatial variability of rainfall in Everest mountain.

Similarily all areas from which the ERA5 data extracted found at different altitudinal level and exhibited variability. Thus, the observed and simulated data showed spatial variability depending on the altitudinal variation, land use land cover and acess to water bodies.

5. Conclusions

The results of the observed data analysis indicated that the rainfall extreme indices were increasing and decreasing at different stations with various rates of change. The south-eastern and north-western parts of the study area experienced contrasting rainfall indices. The average precipitation was 1446.92 mm over the Ghibe III Dam watershed. The rainfall has bimodal patterns, in which the highest amount of rainfall is received in the spring season, followed by the summer season. Seasonal variability of rainfall is higher than annual variability in the study area. Of course, agriculture in developing countries like Ethiopia is more affected by the seasonal variability of rainfall. The areal average temperature maximum and minimum range between 26.4 °C and 13.8 °C, respectively. The dry season (winter) has more inter-annual variability in rainfall and temperature than the Summer, Autumn, and Spring seasons. Most of the months showed a decreasing trend in rainfall and an increasing trend in temperature. The rainfall extremes showed upward and downward trends whereas temperature extremes generally showed a warming trend in the watershed.

Based on the ERA5 climate reanalysis produced by ECMWF, which combines past observations with models to generate consistent time series of multiple climate variables, the seasonal variability of rainfall is higher than the annual variability. Moreover, the PCI (Precipitation Concentration Index), which is a measure of rainfall distribution, showed that about 68 % of the study area had irregular rainfall distribution.

The climate model results also indicated a declining trend in rainfall while an increasing trend in temperature from the base period (1976–2005) to the long term (2071–2100). Besides, the model estimate showed high variability (CV = 20.65 %) in the Climate Limited Area Modeling Community (CCLM) under representative concentration paths (RCP) 4.5 and 8.5 and extremely high variability (CV = 93.49 %) in the Regional Atmospheric Climate Model (RACMO) under RCP 4.5. This study has provided useful information for a better understanding of the nature of the distribution of rainfall and temperature in this specific study area, the Upper Omo Basin, Ghibe III Dam area, which is critical for developing better climate variability adaptive strategies in a changing climate. Furthermore, this finding can be used as a baseline for a larger-scale study of the impact of spatio-temporal rainfall and temperature variability and trends.

Although explanations addressed high and low land in some areas of the study, climatic extreme indices were mostly analyzed at station level in this study. As a result, it was not aggressively included in this study to analyze climatic extreme indices depending on agroecological zones. Of course, this might be considered a limitation. The other limitation is that ERA reanalysis, though expressed in scientific literature as a substitute for observed data and used for bias correction of climate model data, has difficulty of capturing long-term data.

The study is a great example of how policymakers can use scientific research to design effective adaptation strategies for the adverse effects of climate variability. By understanding the seasonal, annual and long-term variability and trends of rainfall and temperature, policymakers can develop area-specific strategies that work for the current study area and areas with similar geographical settings around the world. This can help mitigate the negative impacts of climate change and ensure a sustainable future for all. Further research can replicate the study, which would be better suited to address adverse climate variability and trends at global scale.

Ethics statement

A letter of permission was received from the graduate school of Arba Minch University and given to the Ethiopian metrological agency and Ministry of Water, Electricity, and Energy of Ethiopia to get daily rainfall and temperature data for stations in the Gibe III Dam watershed, southern Ethiopia.

Funding statment

This research didnot receive any grants from funding agencies or organizations

Data availability statement

Data are available based on reasonable request by the author. However, the data associated with our study has not been deposited in a publicly available repository.

CRediT authorship contribution statement

Zewde Sufara Yagaso: Writing – original draft, Validation, Software, Methodology, Investigation, Formal analysis, Data curation, Conceptualization. **Teshome Yirgu Bayu:** Writing – review & editing, Visualization, Validation, Supervision, Methodology, Formal analysis, Data curation, Conceptualization. **Mulugeta Debele Bedane:** Writing – review & editing, Visualization, Validation, Supervision, Methodology, Formal analysis, Data curation, Conceptualization.

Declaration of competing interest

The authors state that they have no known competing financial interests or personal relationships that could have an impact on the work reported in this study.

Acknowledgments

We acknowledge the ERA 5 and CORDEX RCM data sources for making the dataset available for free. We also appreciate the National Meteorological Agency of Ethiopia for supplying free weather station data for rainfall and temperature extreme event analysis, bias correction, and model validation of satellite-based data in our study area. Last but not least, we are grateful to our friends and colleagues for helping us to strengthen our work.

References

[1] M. Almazroui, F. Saeed, S. Saeed, M.N. Islam, M. Ismail, Projected change in temperature and precipitation over Africa from CMIP6, Earth Syst. Environ. 4 (3) (2020) 455–475, https://doi.org/10.1007/s41748-020-00161-x.
[2] A.A. Mekonen, A.B. Berlie, Spatiotemporal variability and trends of rainfall and temperature in the Northeastern Highlands of Ethiopia, Model. Earth Syst. Environ. 6 (1) (2020) 285–300, https://doi.org/10.1007/s40808-019-00678-9.
[3] G. Fufa, S. Addisu, Temperature and precipitation trends using CMIP6 model data using the different senarios in jimma zone , ONRS of Ethiopia, J. Resour. Dev. Manag. 79 (2422–8397) (2021) 13–20, https://doi.org/10.7176/JRDM/79-02.
[4] M.K. Zegeye, K.T. Bekitie, D.N. Hailu, Spatio - temporal variability and trends of hydroclimatic variables at zarima sub - basin north western Ethiopia, Environ. Syst. Res. 11 (27) (2022) 1–21, https://doi.org/10.1186/s40068-022-00273-5.
[5] H. Birara, R.P. Pandey, S.K. Mishra, Trend and Variability Analysis of Rainfall and Temperature in the Tana Basin Region , Ethiopia, 2018, pp. 555–569, https://doi.org/10.2166/wcc.2018.080.
[6] M.A. Worku, G.L. Feyisa, K.T. Beketie, E. Garbolino, Rainfall variability and trends in the Borana zone of southern Ethiopia, J. Water Clim. Chang. 13 (8) (2022) 2–21, https://doi.org/10.2166/wcc.2022.173.
[7] S. Gummadi, et al., Spatio-temporal variability and trends of precipitation and extreme rainfall events in Ethiopia in 1980–2010, Theor. Appl. Climatol. 134 (3–4) (2018) 2–15, https://doi.org/10.1007/s00704-017-2340-1.
[8] V.M. Gálfi, V. Lucarini, J. Wouters, A large deviation theory-based analysis of heat waves and cold spells in a simplified model of the general circulation of the atmosphere, J. Stat. Mech. Theor. Exp. 2019 (3) (2019) 5, https://doi.org/10.1088/1742-5468/ab02e8.
[9] V.M. Gálfi, V. Lucarini, F. Ragone, J. Wouters, Applications of large deviation theory in geophysical fluid dynamics and climate science, Springer 44 (6) (2021) 291–363, https://doi.org/10.1007/s40766-021-00020-z.
[10] M. Jothimani, A. Abebe, Z. Dawit, Mapping of soil erosion-prone sub-watersheds through drainage morphometric analysis and weighted sum approach: a case study of the Kulfo River basin, Rift valley, Arba Minch, Southern Ethiopia, Model. Earth Syst. Environ. 6 (4) (2020) 1–13, https://doi.org/10.1007/s40808-020-00820-y.
[11] G.B. Wubaye, et al., Trends in rainfall and temperature extremes in Ethiopia: station and agro-ecological zone levels of analysis, Atmosphere 14 (3) (2023) 1–24, https://doi.org/10.3390/atmos14030483.
[12] A. Alemayehu, M. Maru, W. Bewket, M. Assen, Spatiotemporal variability and trends in rainfall and temperature in Alwero watershed , western Ethiopia, Environ. Syst. Res. 9 (22) (2020) 1–15, https://doi.org/10.1186/s40068-020-00184-3.
[13] F.A. Anose, K.T. Beketie, T. Terefe Zeleke, D. Yayeh Ayal, G. Legese Feyisa, Spatio-temporal hydro-climate variability in Omo-Gibe river Basin, Ethiopia, Clim. Serv. 24 (December) (2021), https://doi.org/10.1016/j.cliser.2021.100277.
[14] D. Ademe, B.F. Ziatchik, K. Tesfaye, B. Simane, G. Alemayehu, E. Adgo, Climate trends and variability at adaptation scale: patterns and perceptions in an agricultural region of the Ethiopian Highlands, Weather Clim. Extrem. 29 (2020) 100263, https://doi.org/10.1016/j.wace.2020.100263.
[15] M.M. Alemu, G.T. Bawoke, Analysis of spatial variability and temporal trends of rainfall in Amhara Region, Ethiopia, J. Water Clim. Chang. 11 (4) (2020) 1505–1520, https://doi.org/10.2166/wcc.2019.084.
[16] D.Y. Ayal, W. Leal Filho, Farmers' perceptions of climate variability and its adverse impacts on crop and livestock production in Ethiopia, J. Arid Environ. 140 (2017) 20–28, https://doi.org/10.1016/j.jaridenv.2017.01.007.
[17] M.A. Worku, Rainfall variability and trends in the Borana zone of southern Ethiopia, J. water Clim. chnage 13 (8) (2022) 3132–3151, https://doi.org/10.2166/wcc.2022.173.
[18] K. Koudahe, A.J. Kayode, A.O. Samson, A.A. Adebola, K. Djaman, Trend analysis in standardized precipitation index and standardized anomaly index in the context of climate change in southern Togo, Atmos. Clim. Sci. 7 (4) (2017) 401–423, https://doi.org/10.4236/acs.2017.74030.
[19] A. Kawo, R. Van Malderen, E. Pottiaux, B. Van Schaeybroeck, Understanding the present-day spatiotemporal variability of precipitable water vapor over Ethiopia: a comparative study between ERA5 and gps, Rem. Sens. 14 (3) (2022) 2–20, https://doi.org/10.3390/rs14030686.
[20] B. McNicholl, Y.H. Lee, A.G. Campbell, S. Dev, Evaluating the reliability of air temperature from ERA5 reanalysis data, Geosci. Rem. Sens. Lett. IEEE 19 (Xx) (2022) 1–5, https://doi.org/10.1109/LGRS.2021.3137643.
[21] M.E. Shongwe, C. Lennard, B. Liebmann, E.A. Kalognomou, L. Ntsangwane, I. Pinto, An evaluation of CORDEX regional climate models in simulating precipitation over Southern Africa, Atmos. Sci. Lett. 16 (3) (2015) 199–207, https://doi.org/10.1002/ASL2.538.
[22] S. Van Vooren, B. Van Schaeybroeck, J. Nyssen, M. Van Ginderachter, P. Termonia, Evaluation of CORDEX rainfall in northwest Ethiopia: sensitivity to the model representation of the orography, Int. J. Climatol. 39 (5) (2019) 1–18, https://doi.org/10.1002/joc.5971.
[23] D. Jaweso, B. Abate, A. Bauwe, B. Lennartz, Hydro-meteorological trends in the upper Omo-Ghibe river basin, Ethiopia, Water (Switzerland) 11 (9) (2019) 1–18, https://doi.org/10.3390/w11091951.
[24] M. Bekele, T. Mulugeta, D. Belete, M. Dananto, Trends in climatic and hydrological parameters in the ajora - woybo watershed , Omo - Gibe River basin , Ethiopia, SN Appl. Sci. 5 (45) (2023) 1–17, https://doi.org/10.1007/s42452-022-05270-y.
[25] F. Girma, K. Getahun, A. Babu, Assessment of physical land suitability for surface irrigation by using GIS and RS, in case of loma district, south western Ethiopia, Int. J. Curr. Res. Acad. Rev. 7 (1) (2019) 32–45, https://doi.org/10.20546/ijcrar.2019.701.004.

[26] A.E. Selase, D.E.E. Agyimpomaa, D.D. Selasi, D.M.N. Hakii, Precipitation and rainfall types with their characteristic features, J. Nat. Sci. Res. 5 (20) (2015) 89–92 [Online]. Available: https://www.iiste.org/Journals/index.php/JNSR/article/view/26509.
[27] C.G. Jones, et al., Tellus A : Dynamic Meteorology and Oceanography Regional Climate Modelling at the Rossby Centre Regional Climate Modelling at the Rossby Centre, 870, 2011, 2016, https://doi.org/10.1111/j.1600-0870.2010.00491.x.
[28] S.L. Sørland, R. Brogli, P.K. Pothapakula, E. Russo, J. Van De Walle, COSMO-CLM regional climate simulations in the Coordinated Regional Climate Downscaling Experiment (CORDEX) framework : a review, Geosci. Model Dev. (GMD) 14 (5125–5154) (2021) 1–30, https://doi.org/10.5194/gmd-14-5125-2021.
[29] E. van Meijgaard, L.H. Van Ulft, F.C. Bosveld, G. Lenderink, a P. Siebesma, The KNMI Regional Atmospheric Climate Model RACMO, 2008, p. 43. *Tech. report*; TR - 302, version 2.1.
[30] D. Jacob, et al., Assessing the transferability of the regional climate model, Atmosphere 3 (2012) 181–199, https://doi.org/10.3390/atmos3010181.
[31] S. Gleixner, T. Demissie, G.T. Diro, Did ERA5 improve temperature and precipitation reanalysis over East Africa? Atmosphere 11 (9) (2020) 1–19, https://doi.org/10.3390/atmos11090996.
[32] D.T. Reda, A.N. Engida, D.H. Asfaw, R. Hamdi, Analysis of precipitation based on ensembles of regional climate model simulations and observational databases over Ethiopia for the period 1989-2008, Int. J. Climatol. 35 (6) (2015) 948–971, https://doi.org/10.1002/joc.4029.
[33] M. Achite, T. Caloiero, A. Wał, N. Krakauer, Analysis of the spatiotemporal annual rainfall variability in the wadi cheliff basin (Algeria) over the period 1970 to 2018, Water 13 (1477) (2021) 1–9, https://doi.org/10.3390/w13111477.
[34] A.A.S.N. De Campos Ferreira, L.R.B. Dourado, D. Biagiotti, N.P. Da Silva Santos, D.C.N. Nascimento, K.R.S. Sousa, Methods for classifying coefficients of variation in experimentation with poultrys, Comun. Sci. 9 (4) (2018) 565–574, https://doi.org/10.14295/cs.v9i4.2619.
[35] A. Asfaw, B. Simane, A. Hassen, A. Bantider, Variability and time series trend analysis of rainfall and temperature in northcentral Ethiopia : a case study in Woleka sub-basin, Weather Clim. Extrem. 19 (December 2017) (2018) 29–41, https://doi.org/10.1016/j.wace.2017.12.002.
[36] A. Salhi, et al., Rainfall distribution and trends of the daily precipitation concentration index in northern Morocco: a need for an adaptive environmental policy, SN Appl. Sci. 1 (3) (2019) 1–15, https://doi.org/10.1007/s42452-019-0290-1.
[37] C. Ngongondo, C. Xu, L. Gottschalk, Evaluation of Spatial and Temporal Characteristics of Rainfall in Malawi : a Case of Data Scarce Region, 2011, pp. 79–93, https://doi.org/10.1007/s00704-011-0413-0.
[38] K.H. Hamed, A.R. Rao, A modified Mann-Kendall trend test for autocorrelated data, J. Hydrol. 204 (1998) 182–196.
[39] K.A. Elzopy, A.K. Chaturvedi, K.M. Chandran, K. Naveena, U. Surendran, Trend analysis of long-term rainfall and temperature data for Ethiopia, S. Afr. Geogr. J. 00 (00) (2020) 1–14, https://doi.org/10.1080/03736245.2020.1835699.
[40] S. Alashan, Combination of modified Mann-Kendall method and Şen innovative trend analysis, Eng. Reports 2 (3) (2020) 1–13, https://doi.org/10.1002/eng2.12131.
[41] J. Ali Mohammed, T. Gashaw, G. Worku Tefera, Y.T. Dile, A.W. Worqlul, S. Addisu, Changes in observed rainfall and temperature extremes in the upper Blue Nile Basin of Ethiopia, Weather Clim. Extrem. 37 (December 2021) (2022) 100468, https://doi.org/10.1016/j.wace.2022.100468.
[42] S.M. Pingale, D. Khare, M.K. Jat, J. Adamowski, Spatial and temporal trends of mean and extreme rainfall and temperature for the 33 urban centers of the arid and semi-arid state of Rajasthan, India, Atmos. Res. 138 (2014) 73–90, https://doi.org/10.1016/j.atmosres.2013.10.024.
[43] T. Woldemariam Tesfaye, C.T. Dhanya, A.K. Gosain, Evaluation of ERA-interim, MERRA, NCEP-DOE R2 and CFSR reanalysis precipitation data using gauge observation over Ethiopia for a period of 33 years, AIMS Environ. Sci. 4 (4) (2017) 596–620, https://doi.org/10.3934/environsci.2017.4.596.
[44] G. Worku, E. Teferi, A. Bantider, Y.T. Dile, M.T. Taye, Evaluation of regional climate models performance in simulating rainfall climatology of Jemma sub-basin, Upper Blue Nile Basin, Ethiopia, Dynam. Atmos. Oceans 83 (June) (2018) 53–63, https://doi.org/10.1016/j.dynatmoce.2018.06.002.
[45] T.A. Gado, M.B. Mohameden, I.M.H. Rashwan, Bias correction of regional climate model simulations for the impact assessment of the climate change in Egypt, Environ. Sci. Pollut. Res. 29 (2022) 3–21, https://doi.org/10.1007/s11356-021-17189-9, 20200–20220.
[46] Y. Li, B. Guo, K. Wang, G. Wu, Performance of TRMM product in quantifying frequency and intensity of precipitation during daytime and nighttime across China, Rem. Sens. 12 (740) (2020) 1–23, https://doi.org/10.3390/rs12040740.
[47] R. Urraca, T. Huld, A. Gracia-Amillo, F.J. Martinez-de-Pison, F. Kaspar, A. Sanz-Garcia, Evaluation of global horizontal irradiance estimates from ERA5 and COSMO-REA6 reanalyses using ground and satellite-based data, Sol. Energy 164 (February) (2018) 339–354, https://doi.org/10.1016/j.solener.2018.02.059.
[48] E. Mutayoba, J.J. Kashaigili, Evaluation for the Performance of the CORDEX Regional Climate Models in Simulating Rainfall Characteristics over Mbarali River Catchment in the Rufiji Basin , Tanzania, 2017, pp. 139–151, https://doi.org/10.4236/gep.2017.54011.
[49] T.A. Demissie, C.H. Sime, Assessment of the performance of CORDEX regional climate models in simulating rainfall and air temperature over southwest Ethiopia, Heliyon 7 (8) (2021) e07791, https://doi.org/10.1016/j.heliyon.2021.e07791.
[50] N.U. Benson, C. Nwokike, A.B. Williams, A.E. Adedapo, O.H. Fred-Ahmadu, Spatial and temporal trends in diurnal temperature and precipitation extremes in North Central Nigeria, J. Phys. Conf. Ser. 1299 (1) (2019) 2–11, https://doi.org/10.1088/1742-6596/1299/1/012062.
[51] A. Likinaw, A.Alemayehu and W. Bewket, "Trends in Extreme Precipitation Indices in Northwest Ethiopia : Comparative Analysis Using the Mann – Kendall and Innovative," Climate, vol. 11, no. 8, p. 164, doi:https://doi.org/10.3390/cli11080164.
[52] J. Ali, T. Gashaw, G. Worku, Y.T. Dile, A.W. Worqlul, S. Addisu, Changes in observed rainfall and temperature extremes in the upper Blue Nile Basin of Ethiopia, Weather Clim. Extrem. 37 (December 2021) (2022) 100468, https://doi.org/10.1016/j.wace.2022.100468.
[53] F. Chiaravalloti, T. Caloiero, R. Coscarelli, The long-term ERA5 data series for trend analysis of rainfall in Italy, Hydrology 9 (2) (2022) 1–14, https://doi.org/10.3390/hydrology9020018.
[54] A. Arega, M. Arega, B. Berlie, Spatiotemporal variability and trends of rainfall and temperature in the Northeastern Highlands of Ethiopia, Model. Earth Syst. Environ. 2009 (2019), https://doi.org/10.1007/s40808-019-00678-9.
[55] G. Bayable, G. Amare, G. Alemu, T. Gashaw, Spatiotemporal variability and trends of rainfall and its association with pacific ocean sea surface temperature in west harerge zone, eastern Ethiopia, Environ. Syst. Res. 10 (1) (2021) 2–30, https://doi.org/10.1186/s40068-020-00216-y.
[56] A.S. Nannawo, T.K. Lohani, A.A. Eshete, Groundwater recharge evaluation due to climate change using WetSpass-M distributed hydrological model in Bilate river basin of Ethiopia, Groundw. Sustain. Dev. 19 (October) (2022) 9–17, https://doi.org/10.1016/j.gsd.2022.100860.
[57] J.W. Mugo, F.J. Opijah, J. Ngaina, F. Karanja, M. Mburu, Rainfall variability under present and future climate scenarios using the rossby center bias-corrected regional climate model, Am. J. Clim. Change 9 (2020) 243–265, https://doi.org/10.4236/ajcc.2020.93016.
[58] H. Teshome, K. Tesfaye, N. Dechassa, T. Tana, M. Huber, Analysis of past and projected trends of rainfall and temperature parameters in eastern and western Hararghe zones, Ethiopia, Atmosphere 13 (1) (2022) 1–18, https://doi.org/10.3390/atmos13010067.
[59] A.T. Ayalew, The synergic effects of climate variability on rainfall distribution over Hare catchment of Ethiopia, Adv. Meteorol. 2023 (2023) 1–20.
[60] T.D. Geleta, D.K. Dadi, C. Funk, W. Garedew, D. Eyelade, A. Worku, Downscaled climate change projections in urban centers of southwest Ethiopia using CORDEX Africa simulations, MDPI 10 (2022) 158.
[61] J. Eeckman, et al., Providing a non-deterministic representation of spatial variability of precipitation in the Everest region, Hydrol. Earth Syst. Sci. 21 (2017) 4879–4893.